

¹H and ¹³C NMR Study on Local Dynamics of Poly(vinyl alcohol) in Aqueous Solutions

J.-M. Petit and X. X. Zhu*

Département de chimie, Université de Montréal, C.P. 6128, succursale Centre-ville, Montréal, Québec, Canada H3C 3J7

Received October 6, 1995; Revised Manuscript Received December 17, 1995[®]

ABSTRACT: To study the local dynamics of poly(vinyl alcohol) (PVA) in aqueous solutions, several relevant physical models for NMR spin–lattice relaxation in polymers have been tested for ¹³C spin–lattice relaxation times, T_{1C} , nuclear Overhauser enhancement factor, η , determined at 100.6 MHz, and effective ¹H spin–lattice relaxation times, T_1^{eff} , measured at 80, 300, and 400 MHz over a temperature range 5–87 °C. The fitting parameters of the models were obtained from the ¹³C NMR relaxation data, and the their validity was then tested by fitting the parameters to the ¹H relaxation data. The autocorrelation function of Dejean de la Batie et al. (*Macromolecules* **1988**, *21*, 2045) provided the best fit to the data of the PVA–water system studied, showing that the local motion of the polymer could be interpreted by conformational jumps of the backbone and by a fast, anisotropic reorientation movement of the C–H bonds. An AX₂ system was used successfully for the interpretation of the ¹H relaxation data, indicating that dipolar interactions between the hydroxyl group and the protons of the polymer backbone are negligible. An energy barrier associated with the segmental motion of PVA was also estimated (13.4 kJ/mol).

Introduction

Poly(vinyl alcohol) (PVA) is a common polymer that, in its gel state in water, finds many industrial and biomedical applications.^{1,2} Due to the existence of inter- and intramolecular hydrogen bonds, a solution of PVA in water can become a gel, as predicted by the value of the Flory–Huggins parameter, χ , which is 0.49 at 30 °C.³ The dynamic behavior of PVA in aqueous solutions is particularly interesting because it shows complex solution properties.^{1,2} For example, an understanding of polymer dynamics should be useful in the interpretation of the diffusion behavior of the probe molecules in these systems.^{4,5}

To study the local dynamics of a polymer chain, nuclear magnetic resonance (NMR) spectroscopy has proved to be a powerful tool because its selectivity allows one to probe specific groups at the atomic level to analyze the motions of the polymer chain. Moreover, spin–lattice relaxation in ¹H and ¹³C NMR provides information on very rapid processes as well as on much slower modes. Spin–lattice relaxation arises almost entirely from intramolecular dipole–dipole interactions modulated by the general polymer motion. In the case of ¹³C relaxation, the situation is relatively simple since one has only to consider the C–H nuclear dipole, but for proton relaxation one has to consider interactions with all of the proton's nearest neighbors on the chain, while intermolecular contributions to polymer relaxation are negligible.⁶ Since protons are on the periphery of the polymer chain, they should be more sensitive to the conformational change or motion of the polymer chain in NMR studies.

Relaxation parameters are governed by the spectral density function, $J(\omega)$, which is defined from the autocorrelation function, $G(\tau)$:

$$J(\omega) = \int_{-\infty}^{+\infty} G(\tau) e^{i\omega\tau} d\tau \quad (1)$$

where $G(\tau)$ is the normalized second-order spherical

harmonic autocorrelation function.⁷ Such a function describes the persistence of a dynamic process before being averaged out by the molecular motion in solution and is related to a correlation time τ_c for the molecular motions. $J(\omega)$ gives the intensity of the molecular motions at a frequency ω . To fully determine the polymer motion, it is desirable to measure the autocorrelation function $G(\tau)$, but NMR relaxation measurements provide only a few points in the frequency domain via $J(\omega)$. The well-known description of the isotropic rotation characterized by one correlation time given by Bloembergen et al.⁸ cannot apply to polymers because fast bond oscillations or local conformational changes and rotation of the whole chain due to much slower modes all take place in polymer solutions.^{9–13}

To interpret the experimental data, two very different approaches have been used to derive autocorrelation functions applicable to flexible polymer chains. One is purely phenomenological. It assumes that the rigid-rotor model may be used for describing elementary modes of motion, each characterized by a correlation time τ_c . Hence, the spectral density function, $J(\omega)$, is obtained by averaging eq 1 over all values of τ by means of a distribution function.¹⁴ Empirical distributions with two adjustable parameters have been proposed along this line.^{9,10,14} The second and perhaps more satisfying approach is based on the search for a relevant molecular model capable of describing the local backbone motions of a flexible chain. Along this line, Valeur et al. developed a model based on conformational jumps articulated on a tetrahedral lattice.¹⁵ This model, as well as alternative forms of it by Jones and Stockmayer¹⁶ and by Hall and Helfand,¹⁷ contains two adjustable parameters for the expression of $G(\tau)$. In these models, the two parameters are correlation times associated with different kinds of motion of the chains. The models have been shown to provide acceptable fittings to NMR spin relaxation data of both polymer solutions^{10,13} and rubbery materials.¹⁸ More recently, Dejean de la Batie et al.¹⁹ noted an important failure of the model of Hall and Helfand in the temperature region where T_1 exhibits a minimum. This problem has been shown to be quite general to the conformational

* Author to whom correspondence should be addressed: telephone, (514) 343-6733; fax, (514) 343-7586.

[®] Abstract published in *Advance ACS Abstracts*, February 15, 1996.

jump models. Dejean de la Batie et al. suggested, on the basis of a proposition of Howarth,²⁰ that a fast libration of the C–H bonds may contribute to spin relaxation in addition to the conformational rearrangements along the backbone.

The aim of the present work was to study how the local dynamics of a PVA–water system can be described by these models. This was done by obtaining the relevant parameters of the models from the ¹³C NMR relaxation data of PVA and then verifying the validity of the models by fitting to the ¹H NMR relaxation data. For this purpose, spin–lattice relaxation times and nuclear Overhauser enhancement factors (η) were measured as a function of temperature at one frequency for ¹³C and at several frequencies for ¹H. The testing of several relevant models for the PVA–water systems are discussed in this report, including the log χ^2 distribution proposed by Schaefer,⁹ the conformational jump model derived by Valeur et al.,¹⁵ and the model proposed by Dejean de la Batie et al.¹⁹

Theoretical Background

Spectral Density Functions. The normalized log χ^2 distribution function proposed by Schaefer is written in terms of a variable S , which is a b -base logarithmic function of τ :⁹

$$F(S) = [1/\Gamma(p)] [(pS)^{p-1} p \exp(-pS)] \quad (2)$$

where

$$S = \log_b[1 + (b - 1)(\tau/\tau_0)] \quad (3)$$

τ_0 is the average correlation time corresponding to the mean value of S ($S = 1$), p is a parameter indicating the width of the distribution, and $\Gamma(p)$ is the γ -function of τ . The average value of the spectral density function, $\bar{J}(\omega)$, for a given value of ω can be computed by the following numerical integration:

$$\bar{J}(\omega) = \int_0^{+\infty} [\tau/(1 + \omega^2\tau^2)] G(\tau) d\tau \quad (4)$$

with

$$G(\tau) d\tau = F(S) dS \quad (5)$$

Valeur et al. presented an analytical form of the autocorrelation function, in which the polymer motion is considered to be a combination of conformational jumps, with the backbone carbon atoms confined to a tetrahedral lattice, and overall molecular tumbling. The correlation function can be written as

$$G(\tau) = \exp(-\tau/\tau_0) \exp(\tau/\tau_D) [1 - \text{erf}(\tau/\tau_D)^{1/2}] \quad (6)$$

where τ_D and τ_0 are the correlation times of the conformational jumps and overall tumbling, respectively, and $\text{erf}(x)$ is the function of error. Such an

autocorrelation function yields

$$J(\omega) = \frac{2\tau_D\tau_0(\tau_0 - \tau_D)}{(\tau_0 - \tau_D)^2 + \omega^2\tau_D^2\tau_0^2} \left[\sqrt{\frac{\tau_0}{2\tau_D}} \sqrt{\frac{(1 + \omega^2\tau_0^2)^{1/2} + 1}{1 + \omega^2\tau_0^2}} + \sqrt{\frac{\tau_0}{2\tau_D}} \frac{\omega\tau_0\tau_D}{\tau_0 - \tau_D} \sqrt{\frac{(1 + \omega^2\tau_0^2)^{1/2} - 1}{1 + \omega^2\tau_0^2}} - 1 \right] \quad (7)$$

Another conformational jump model by Hall and Helfand¹⁷ has two distinct correlation times as adjustable parameters. The autocorrelation function is given by

$$G(\tau) = \exp(-\tau/\tau_2) \exp(-\tau/\tau_1) I_0(\tau/\tau_1) \quad (8)$$

where I_0 is the modified Bessel function of zero order and τ_1 and τ_2 are the correlation times corresponding to the cooperative and single-bond rearrangements, respectively. Dejean de la Batie et al. have also suggested an alternative interpretation of the correlation time τ_2 in terms of a damping factor for cooperative motion. They modified this last model with the assumption of an additional motion of the C–H vectors about their equilibrium conformation, which is defined as a random anisotropic fast reorientation of the C–H vector inside a cone of half-angle θ , the axis of which is the rest position of the C–H bond. By assuming first that this motion is independent of the conformational rearrangements and second that its correlation time, τ_L , is much shorter than that of the fast motion, Dejean de la Batie et al. derived the following expression for $G(\tau)$:

$$G(\tau) = (1 - a) \exp(-\tau/\tau_2) \exp(-\tau/\tau_1) I_0(\tau/\tau_1) + a \exp(-\tau/\tau_L) \quad (9)$$

where

$$1 - a = [\cos \theta (1 + \cos \theta)]^2/4 \quad (10)$$

The Fourier transform of eq 9 is the spectral density function:

$$J(\omega) = 2(1 - a) \text{Re} \left(\frac{1}{(\alpha + i\beta)^{1/2}} \right) + a \frac{2\tau_L}{1 + \omega^2\tau_L^2} \quad (11)$$

with

$$\alpha = \tau_2^{-2} + 2\tau_1^{-1}\tau_2^{-1} - \omega^2 \quad (12)$$

and

$$\beta = 2\omega (\tau_1^{-1} + \tau_2^{-1}) \quad (13)$$

¹³C Relaxation Parameters. With the assumption of a purely ¹³C–¹H dipolar relaxation mechanism, the spin–lattice relaxation time T_{1C} obtained from a ¹³C experiment is given by the well-known expression²¹

$$\frac{1}{nT_{1C}} = \frac{\gamma_C^2 \gamma_H^2 \hbar^2}{20r_{CH}^6} [J(\omega_H - \omega_C) + 3J(\omega_C) + 6J(\omega_H + \omega_C)] \quad (14)$$

where \hbar is Planck's constant divided by 2π , γ_C and γ_H are the magnetogyric ratios of ¹³C and ¹H nuclei,

respectively, n is the number of directly bonded protons, ω_C and ω_H are the ^1H and ^{13}C resonance frequencies, and r_{CH} is the C–H bond length (1.09 Å). Since ω_C and ω_H differ by a factor of 4, measurements of $T_{1\text{C}}$ sample $J(\omega)$ in the megahertz region.

The nuclear Overhauser enhancement factor, η , is given by²¹

$$\eta = \frac{\gamma_H}{\gamma_C} \frac{6J(\omega_H + \omega_C) - J(\omega_H - \omega_C)}{J(\omega_H - \omega_C) + 3J(\omega_C) + 6J(\omega_H + \omega_C)} \quad (15)$$

^1H Relaxation Parameters for an AX_2 System.

Heatley and Cox²² have been able to interpret ^1H relaxation data in vinyl polymers, particularly for poly(vinyl acetate) in toluene, by assuming that there are no dipolar interactions between the backbone protons and the side groups. If S_A and S_X represent the total methine and methylene longitudinal magnetizations, respectively, then the spin–lattice relaxation is governed by²³

$$\frac{dS_i}{dt} = \sum_{j=\text{A,X}} R_{ij}(S_j - S_j^0) \quad (16)$$

where the subscripts i and j denote the protons A and X, S_j^0 is the value of the longitudinal magnetization at thermal equilibrium, and $R_{ij} = 1/T_{ij}$ are the cross-relaxation rates. In the case of dipolar interactions, and by assuming only intramolecular contributions to the relaxation, the cross-relaxation rates are given by

$$\frac{1}{T_{\text{AA}}} = 6K \left(\frac{J(\omega_A) + 4J(2\omega_A)}{r_{\text{AA}}^6} \right) + 4K \left(\frac{J(\omega_A - \omega_X) + 3J(\omega_A) + 6J(\omega_A + \omega_X)}{r_{\text{AX}}^6} \right)$$

$$\frac{1}{T_{\text{XX}}} = 3K \left(\frac{J(\omega_X) + 4J(2\omega_X)}{r_{\text{XX}}^6} \right) + 2K \left(\frac{J(\omega_A - \omega_X) + 3J(\omega_A) + 6J(\omega_A + \omega_X)}{r_{\text{AX}}^6} \right)$$

$$\frac{1}{T_{\text{AX}}} = \frac{1}{2T_{\text{XA}}} = 2K \left(\frac{6J(\omega_A + \omega_X) - J(\omega_A - \omega_X)}{r_{\text{AX}}^6} \right)$$

where $K \gamma_H^4 \hbar / 20$ and r_{AA} , r_{AX} , and r_{XX} are the effective A–A, A–X, and X–X distances defined by

$$\frac{1}{r_{\text{AA}}^6} = \left(\frac{1}{r_{\text{AA}}^{(1)}} \right)^6 + \left(\frac{1}{r_{\text{AA}}^{(2)}} \right)^6 + \left(\frac{1}{r_{\text{AA}}^{(3)}} \right)^6 + \dots$$

where $r_{\text{AA}}^{(1)}$ is the average distance between nearest neighboring methine protons, $r_{\text{AA}}^{(2)}$ is the average distance between next nearest protons, and so on. r_{AX} is defined in the same way as r_{AA} . r_{XX} is calculated in a different way because of the geminal methylene protons:

$$\frac{1}{r_{\text{XX}}^6} = \left(\frac{1}{r_{\text{XX}}^g} \right)^6 + 4 \left[\left(\frac{1}{r_{\text{XX}}^{(1)}} \right)^6 + \left(\frac{1}{r_{\text{XX}}^{(2)}} \right)^6 + \dots \right]$$

where r_{XX}^g is the distance between the geminal methylene protons, $r_{\text{XX}}^{(1)}$ is the average distance between

nearest neighboring methylene protons, and so on. The determination of these distances is described later.

The recovery of S_A and S_X is governed by the coupled differential equation (eq 16). For a standard inversion recovery technique using the π – t – $\pi/2$ pulse sequence with no perturbing fields, solutions of these equations yield

$$S_A^0 - S_A = P \exp(-t/T_+) + Q \exp(-t/T_-)$$

$$S_X^0 - S_X = P' \exp(-t/T_+) + Q' \exp(-t/T_-) \quad (17)$$

where the variables T_+ , T_- , P , Q , P' , and Q' can be calculated from the following equations:

$$\frac{1}{T_{\pm}} = \frac{1}{2} \left\{ \left(\frac{1}{T_{\text{AA}}} + \frac{1}{T_{\text{XX}}} \right) \pm \left[\left(\frac{1}{T_{\text{AA}}} + \frac{1}{T_{\text{XX}}} \right)^2 - 4 \left(\frac{1}{T_{\text{AA}} T_{\text{XX}}} - \frac{1}{T_{\text{AX}} T_{\text{XA}}} \right) \right]^{1/2} \right\}$$

$$P = \frac{2S_A^0(T_{\text{AX}}/T_- - T_{\text{AX}}/T_{\text{AA}}) - 2S_X^0}{(T_{\text{AX}}/T_+ - T_{\text{AX}}/T_-)}$$

$$P' = P(T_{\text{AX}}/T_+ - T_{\text{AX}}/T_{\text{AA}})$$

$$Q = \frac{2S_A^0(T_{\text{AX}}/T_+ - T_{\text{AX}}/T_{\text{AA}}) - 2S_X^0}{(T_{\text{AX}}/T_- - T_{\text{AX}}/T_+)}$$

$$Q' = Q(T_{\text{AX}}/T_- - T_{\text{AX}}/T_{\text{AA}})$$

In principle, the recovery of S_A and S_X is nonexponential, but previous studies carried out by Scrivens and Heatley²⁴ on AX_2 systems of small molecules have shown that when $r_{\text{AX}}/r_{\text{XX}} > 1.3$, as is the case here, the recovery is described by a single exponential with effective relaxation times, T_1^{eff} . This was confirmed by the experimental results described in the following and by other studies on vinyl polymers.^{22,25}

Experimental Section

Materials. PVA of molecular weight 50 000 and degree of hydrolysis 99% was purchased from Aldrich (Milwaukee, WI), and D_2O (99.9% D) was from C.I.L. (Woburn, MA). The samples were prepared gravimetrically: PVA and water were weighed directly into 5- or 10-mm NMR tubes, which were then sealed to prevent the loss of volatile components. The PVA concentration was 15% unless specified otherwise. The samples were heated for 5 h at 100–110 °C and the measurements were made within 2 days to prevent gelation. Otherwise, the samples were heated for an hour at 100 °C before the experiment. This treatment provided as reproducible results as the fresh samples.

^{13}C NMR Measurements. $T_{1\text{C}}$ measurements were carried out under scalar decoupling on a Bruker ARX-400 spectrometer operating at 100.6 MHz for ^{13}C by using the standard inversion–recovery Fourier transform technique (IRFT). The spectral width and digital resolution were 80 kHz and 0.5 Hz/point, respectively. The pulse delay time, PD, in the IRFT sequence (π – t – $\pi/2$ –AT–PD) was always set longer than 5 times the longest $T_{1\text{C}}$ among those to be simultaneously determined. The data acquisition time, AT, was constant at 1 s. At least 10 values of the delay time t in the range 0–1.5 $T_{1\text{C}}$ were selected for each measurement. The individual $T_{1\text{C}}$ values were computed from the nonlinear regression analysis of the decrease in $(S_{\infty} - S_t)$ as a function of t . The nuclear Overhauser enhancements, η , were determined from the intensity ratios of scalar-decoupled and inverse-gated-decoupled spectra. The former were measured with the sequence PD_1 – $\pi/2$ –AT with $\text{PD}_1 > 5 T_{1\text{C}}$, and the latter were

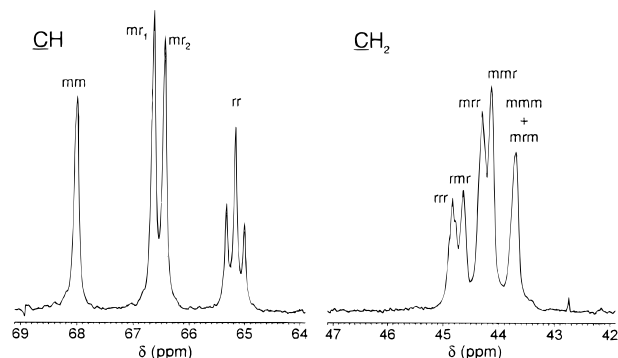


Figure 1. 100.6-MHz proton-decoupled ^{13}C NMR spectrum of PVA in aqueous solution recorded at 60 °C showing the dyad distribution in the methine (CH) region and the tetrad distribution in the methylene (CH_2) region.

Table 1. Observed and Calculated Fractions of Dyad and Tetrad Tacticity of the Poly(vinyl alcohol) Sample

group	sequence	δ (ppm)	fraction	
			observed	calculated ^a
CH	rr	64.8–65.5	0.286	0.286
	mr	66.1–66.9	0.486	0.486
	mm	67.7–68.4	0.227	0.227
CH_2	mmm + mrm	43.4–43.9	0.236	0.110 + 0.111
	mrr	44.0–44.2	0.234	0.235
	mrr	44.2–44.5	0.273	0.262
	rrr	44.5–44.7	0.128	0.126
	rrr	44.7–45.1	0.128	0.155

^a Calculated by using the first-order Markov model with $P_{mr} = 0.517$ and $P_{rm} = 0.460$.

measured with the sequence $\text{PD}_2 - \pi/2 - \text{AT}$ with $\text{PD}_2 > 10T_{1C}$. In the latter sequence, the decoupler was turned off during the pulse delay time PD_2 . Nuclear Overhauser enhancement factor, η , corresponds to the relative increase in intensity due to the Overhauser effect.

^1H NMR Measurements. The ^1H NMR measurements were carried out at 80, 300, and 400 MHz with Bruker WP-80, Varian VXR-300, and Bruker ARX-400 instruments, respectively, by using the IRTF technique. The spectral width was fixed at 6.5 ppm. The decrease in $(S_\infty - S_t)$ as a function of t was fitted to a single exponential, using nonlinear regression analysis to determine T_1^{eff} .

For both ^1H and ^{13}C NMR experiments, T_1 determinations were made with reproducibility within about 10% at each temperature. All chemical shifts were recorded relative to tetramethylsilane set at 0 ppm.

Results and Discussion

Figure 1 shows a 100.6-MHz proton-decoupled ^{13}C spectrum measured at 60 °C for atactic PVA in D_2O . The assignments of the different peaks were made by using Ovenall's results on the microstructure of PVA.²⁶ The tactic sequencing can be described by a first-order Markov model. In the present work, the first-order Markov probabilities, $P_{m/r}$ and $P_{r/m}$, where $P_{m/r}$ is the probability that a growing chain ending in a meso sequence will add a monomer unit to give a racemic sequence, were calculated by equations given by Bovey.²⁷ The fractional areas of the three triad features, *mm*, *mr*, and *rr*, gave $P_{m/r} = 0.517$ ($P_{m/m} = 0.483$) and $P_{r/m} = 0.460$ ($P_{r/r} = 0.540$). The fractional areas of the tetrads of the methylene group were measured by the integral of the spectrum using deconvolution and are compared in Table 1 with predictions of the first-order Markov model as explained by Bovey.²⁷ The behavior of the atactic PVA in D_2O is quasi-Bernoullian ($P_{m/r} = P_{r/m} = P_r$ and $P_{r/m} = P_{m/m} = P_m$) and can be compared with Ovenall's study²⁵ on PVA in dimethyl sulfoxide, from

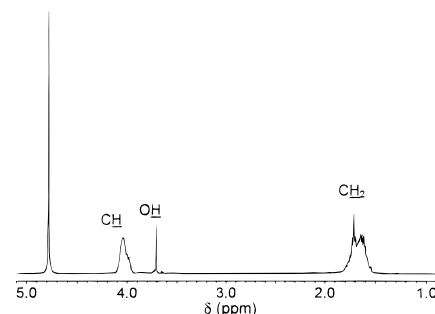


Figure 2. 400-MHz ^1H NMR spectrum of PVA in aqueous solution recorded at room temperature.

which he obtained Bernoullian behavior with $P_m = 0.47$. In the proton spectrum (Figure 2), a multiplet is observed at 1.5–1.9 ppm for CH_2 and a broad peak is seen at 3.9–4.1 ppm for CH at room temperature in D_2O .

By knowing the fractional weight of the different tacticities, one can calculate the distances r_{AX} , r_{AA} , and r_{XX} . There are significant interactions between protons separated by four or five bonds, and the distances $r_{AA}^{(1)}$, $r_{AA}^{(2)}$, $r_{XX}^{(1)}$, etc., were calculated for the six different tetrads in the trans conformation, with a torsional angle of 0°, a C–C bond length of 1.54 Å, a C–H bond length of 1.09 Å, a C–C–C angle of 112°, and a C–C–H angle of 112°. The effective internuclear distances resulting from averaging over tacticity were $r_{AA} = 2.83$ Å, $r_{XX} = 1.63$ Å, and $r_{AX} = 2.38$ Å. Heatley and Cox, in their study of the relaxation of poly(vinyl acetate),²² calculated these distances by taking into account the most favored conformations of the different tetrads and a torsional angle not equal to zero. For r_{AA} , r_{XX} , and r_{AX} , they obtained 2.73, 1.66, and 2.41 Å, respectively. Despite the simplifications made in this work, the distances do not differ from these values by more than 5%.

Experimental results for ^{13}C and ^1H relaxation data are shown in Figures 3 and 4. For the methylene group, only the well-defined peaks associated with *mrr*, and *mrm* + *mmm* sequences allowed the determination of the spin–lattice relaxation times, T_{1C} , of the ^{13}C nucleus in the whole temperature range. As shown in Figure 3A, the effect of the tacticity is not significant, but the value of the $T_{1C}^{\text{CH}}/T_{1C}^{\text{CH}_2}$ ratio in the temperature range of study is different from 2, the value expected from the number of protons directly bonded to each of the carbons considered. A ratio of 1.82 ± 0.08 is obtained, which indicates that the local motions in PVA, as observed by NMR, are not identical for the internuclear vectors associated with the CH and CH_2 carbons.²⁸ ^1H NOE measurements in ^{13}C NMR (Figure 3B) and ^1H relaxation data (Figure 4) show that even at high temperatures the extreme narrowing condition is not reached and that the data correspond, in this temperature range, to the region where the spin–lattice relaxation time goes through a minimum. In the case of a polymer solution, this region is broad due to the more complicated motions of the polymer chains.

The ^{13}C relaxation data allow one to determine the parameters (τ_0, p) and (τ_0, τ_D) of the models of Schaefer and of Valeur et al., respectively. The calculation was accomplished by using the numeric method of Denault,²⁹ eqs 4, 14, and 15 for the model of Schaefer, eqs 7, 14, and 15 for the model of Valeur et al., and the experimental data for the CH peak. The results are reported in Table 2 and were used to simulate the ^1H relaxation

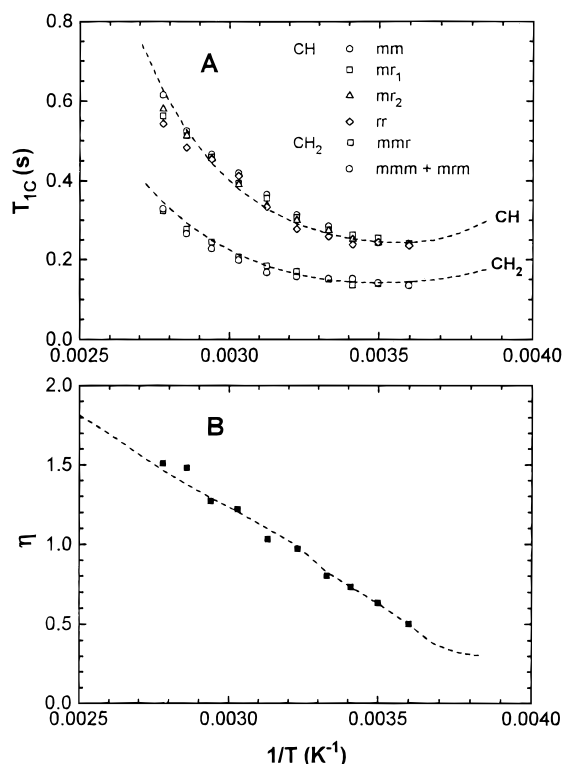


Figure 3. (A) T_{1C} values for the methine and methylene carbons and (B) nuclear Overhauser enhancement factor, η , of PVA measured at 100.6 MHz as a function of reciprocal temperature, $1/T$. Dashed curves correspond to fittings to the model of Dejean de la Batie et al., with $\tau_2/\tau_1 = 10$, $\tau_1/\tau_L = 200$, and $a = 0.21$ for CH carbon and $a = 0.33$ for CH_2 carbon.

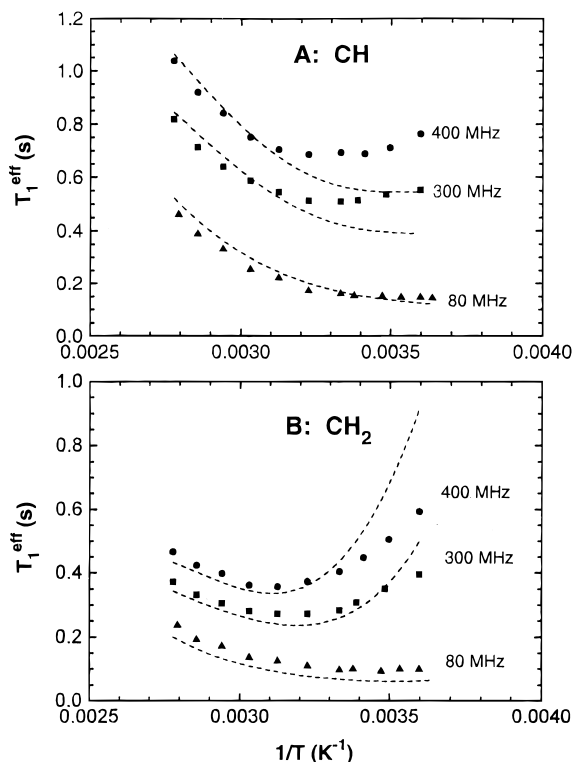


Figure 4. 80-, 300-, and 400-MHz T_1^{eff} values for (A) the methine proton and (B) the methylene proton in PVA solution plotted as a function of reciprocal temperature, $1/T$. Dashed curves correspond to fittings to the model of Dejean de la Batie et al., with $\tau_2/\tau_1 = 10$, $\tau_1/\tau_L = 200$, and $a = 0.21$ for methine carbon and $a = 0.33$ for methylene carbon.

data for different frequencies to test the validity of the models. To simulate the recovery of S_A and S_X , the

Table 2. Parameters for the Different Models Adjusted from ^{13}C Relaxation Data Measured at 100.6 MHz^a

temp (°C)	model of Schaefer		model of Valeur et al.		model of Dejean de la Batie et al. ^b $\log \tau_1$
	$\log \tau_0$	p	$\log \tau_D$	$\log \tau_0$	
5	no solution		no solution		-8.908
13	no solution		-9.045	-8.596	-9.045
20	-9.038	18.52	-9.149	-8.763	-9.150
27	-9.160	16.68	-9.282	-8.811	-9.270
37	-9.520	15.07	-9.582	-8.926	-9.465
47	-9.725	16.60	-9.733	-9.021	-9.625
57	-9.920	20.00	-9.886	-9.129	-9.810
67	-10.03	22.71	-10.020	-9.187	-9.940
77	-10.10	28.13	-10.102	-9.272	-10.06
87	-10.20	31.23	-10.254	-9.345	-10.17

^a Correlation times are in seconds. ^b Calculated by using $\tau_2/\tau_1 = 10$, $\tau_1/\tau_L = 200$, and $a = 0.21$ for CH carbon and $a = 0.33$ for CH_2 carbon.

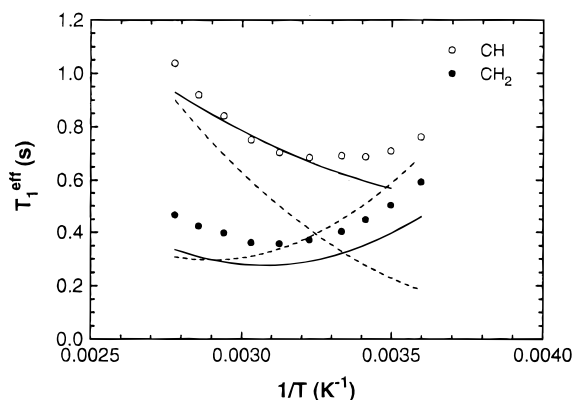


Figure 5. Comparisons of the T_1^{eff} values of the methine and methylene protons at 400 MHz with the predictions of the models of Schaefer (dashed lines) and of Valeur et al. (solid lines). Parameters for both fittings are listed in Table 2.

parameters of eq 17 were calculated for a particular motional model at each temperature studied, and the effective ^1H spin-lattice relaxation times, T_1^{eff} , were determined by fitting the recovery of S_A and S_X to a single-exponential function. Comparisons of the predictions of both models with experimental data are shown in Figure 5 for the 400-MHz frequency. The major inconvenience of these models is that they cannot explain the deviation from the value of 2 of the $T_{1C}^{\text{CH}}/T_{1C}^{\text{CH}_2}$ ratio. Both models, the one of Schaefer describing polymer motion by a distribution of correlation times and the one of Valeur et al. based on conformational jumps, cannot reproduce the ^1H relaxation data at 400 MHz as shown in Figure 5 nor at 80 and 300 MHz as we have verified. However, in this study, the model of Valeur et al. gave a better prediction of the methine protons' spin-lattice relaxation times at high temperatures. For methylene protons, this model gave the correct evolution of the curve in the temperature range considered, although the predicted values are generally lower than the experimental data. On the other hand, the model of Schaefer deviated more significantly from the experimental results.

The model of Dejean de la Batie et al. is based on the conformational jump model of Hall and Helfand¹⁷ and on the assumption of the libration of C-H bonds.²⁰ In this model, the deviation from 2 of the $T_{1C}^{\text{CH}}/T_{1C}^{\text{CH}_2}$ ratio can be explained by the nonidentical motions of the internuclear vectors associated with the CH and CH_2 carbons. In the application of the model, it results in two different libration movements of the CH and CH_2 carbons, characterized by two different values of the

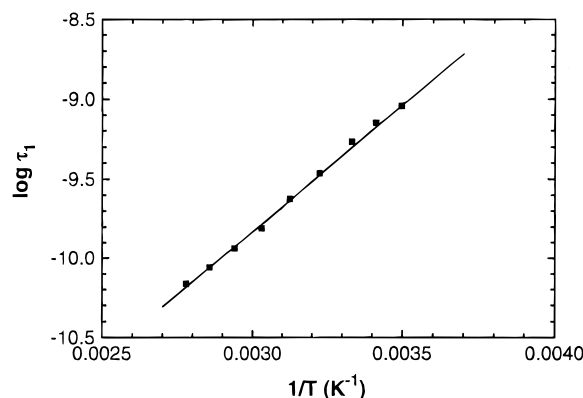


Figure 6. Arrhenius plot of the correlation time τ_1 for the model of Dejean de la Batie et al.

parameter a . The parameters of the model, a , τ_1 , τ_2/τ_1 , and τ_1/τ_L , as introduced by Dejean de la Batie et al., cannot be determined without further assumptions since one may use only ^{13}C spin-lattice relaxation times and the nuclear Overhauser enhancement factor. As in the work by Dejean de la Batie et al., computations were performed by using the following characteristics of the model:¹⁹ (1) the parameters a , τ_2/τ_1 , and τ_1/τ_L are not temperature-dependent; (2) in the temperature range considered in this work, the parameter a has only an amplitude effect on T_{1C} and no effect on η ; and (3) the parameter τ_1/τ_L has no effect on either T_{1C} or η . The parameter τ_1/τ_L was taken as 200, which is a value commonly encountered in linear polymers.³⁰ Both parameters a and τ_2/τ_1 were optimized from ^{13}C spin-lattice relaxation times and nuclear Overhauser enhancement factors with different values for methine and methylene carbons. The results of the optimization are the following: CH, $a = 0.21$, $\tau_2/\tau_1 = 10$, $\tau_1/\tau_L = 200$; CH_2 , $a = 0.33$, $\tau_2/\tau_1 = 10$, $\tau_1/\tau_L = 200$. τ_1 values are reported in Table 2 and plotted as a function of the reciprocal of temperature in Figure 6. The predictions of the model of Dejean de la Batie et al. for ^{13}C relaxation parameters are shown in Figure 3, and the predictions for ^1H spin-lattice relaxation times of PVA are shown in Figure 4. This model gave a good prevision of the ^1H spin-lattice relaxation times at each frequency in the high-temperature region, but a deviation appears for lower temperatures. Two points must be noted. First, we assumed that both correlation times, τ_1 and τ_2 , have the same temperature dependency, which is a simplified treatment of the conformational models. Second, in the region of temperature where $\omega\tau_1 > 1$, which is the region of interest, the spectral density function, $J(\omega)$, depends strongly on the frequency, especially in the hertz domain, and proton spin-lattice relaxation times sample $J(\omega)$ in this domain of frequency. Dejean de la Batie et al. have always tested their autocorrelation function with the help of ^{13}C relaxation parameters in the megahertz domain,^{19,31} where the variations in $J(\omega)$ are minimized.

An Arrhenius plot of the correlation time τ_1 is shown in Figure 6 and allows one to calculate an activation energy for the dynamic process associated with τ_1 in solution, E_{sol} , of 30.9 kJ/mol. This activation energy can be related to an energy barrier, E^* , characterizing the conformational transition of the polymer chain associated with the correlation time τ_1 .³²

$$\tau_1 \approx \eta_0 C \exp(E^*/RT) \quad (18)$$

where η_0 is the solvent viscosity and C is a molecular

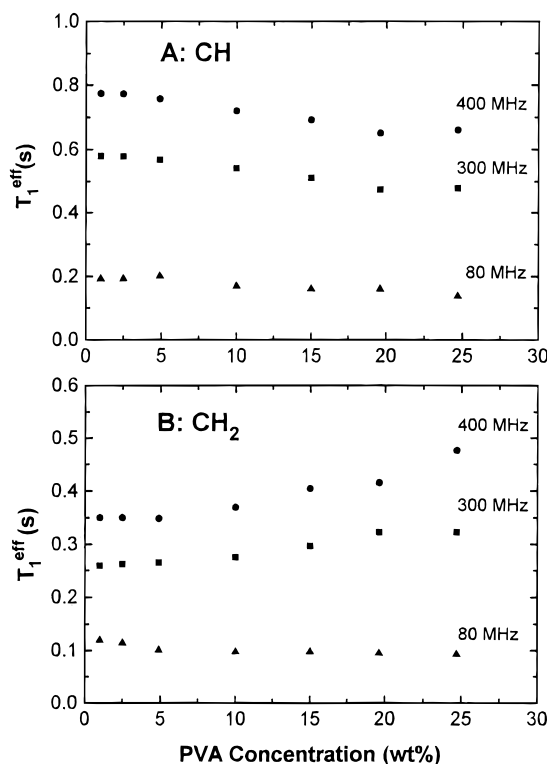


Figure 7. Proton T_1^{eff} values measured at 80, 300, and 400 MHz for (A) the methine and (B) the methylene groups in PVA solutions as a function of polymer concentration.

constant. The activation energy of the motional mode associated with τ_1 can then be estimated from

$$E^* = E_{\text{sol}} - E_{\eta} \quad (19)$$

where E_{η} is the activation energy for the solvent viscosity. For water, $E_{\eta} = 17.5$ kJ/mol in this temperature range.^{33,34} Therefore, the energy barrier associated with the segmental motion of the PVA chain is $E^* = 13.4$ kJ/mol, which is on the order of the rotational energy barrier of the PVA chain (about 11.7 kJ/mol).³⁵

All of the experimental results discussed earlier are based on a PVA-water system with 15 wt % polymer. Figure 7 clearly shows the effect of PVA concentration on the NMR spin-lattice relaxation times of the methine and methylene protons of PVA. Several points can be made from this figure: (1) The dilution of the sample is almost equivalent to an increase in temperature, although it is difficult to correlate the data to any particular temperature range studied. (2) Even at very low concentrations of PVA, the T_1^{eff} values of the protons are dependent on the frequency since they are located close to the minimum, as shown on the figure. (3) The change in T_1^{eff} values of the two kinds of protons as a function of PVA concentration are different, a characteristic of their frequency dependency and another indication that more than one correlation time is needed in the description of local chain dynamics.

Summary and Conclusions

NMR spin-lattice relaxation data can be used to obtain parameters of various physical models. Although the models tested all seem to be able to provide relevant fitting parameters from the ^{13}C relaxation data, verification of the models on the ^1H relaxation data reveals that only the expression of the autocorrelation function of Dejean de la Batie et al. seems to closely fit the data

of the PVA–water system studied and, thus, can be used to interpret the local dynamics of the system. The analysis of the ^1H spin–lattice relaxation times of methine and methylene groups in PVA also indicates that there is no significant dipolar interaction between the hydroxyl protons and the protons of the polymer backbone, which can be taken as evidence of strong hydrogen bonding between the hydroxyl groups of the polymer and the solvent water. An apparent activation energy of the conformational transition was also estimated from the results. In addition, the effect of increasing polymer concentration is approximately equivalent to that of decreasing temperature.

Acknowledgment. We thank the Natural Sciences and Engineering Research Council (NSERC) of Canada and the Quebec Government (Fonds FCAR) for their financial support of this work.

References and Notes

- (1) Peppas, N. A. in *Hydrogels in Medicine and Pharmacy*; Peppas, N. A., Ed.; CRC Press: Boca Raton, FL, 1986; Vol. II, Chapter 1.
- (2) Finch, C. A. *Polyvinyl Alcohol Developments*, 2nd ed.; John Wiley & Sons: Chichester, UK, 1992.
- (3) Brandrup, J.; Immergut, E. H. *Polymer Handbook*, 3rd ed.; John Wiley & Sons: New York, 1989; Section VII, p 177.
- (4) Petit, J.-M.; Zhu, X. X.; Macdonald, P. M. *Macromolecules* **1995**, *29*, 70.
- (5) Phillies, G. D. J. *J. Phys. Chem.* **1989**, *93*, 5029.
- (6) Anderson, J. E.; Liu, K.-J.; Ulman, R. *Discuss. Faraday Soc. (Polym. Phys. Ed.)* **1970**, *49*, 257.
- (7) Abragam, A. *The Principles of Nuclear Magnetism*; Oxford University Press: London, 1961; Chapters 2 and 8.
- (8) Bloembergen, N.; Purcell, E. M.; Pounds, R. V. *Phys. Rev.* **1948**, *73*, 679.
- (9) Schaefer, J. *Macromolecules* **1973**, *6*, 882.
- (10) Heatley, F.; Begum, A. *Polymer* **1976**, *17*, 399.
- (11) Schilling, F. C.; Cais, R. E.; Bovey, F. A. *Macromolecules* **1978**, *11*, 325.
- (12) Jones, A. A.; Bisceglia, M. *Macromolecules* **1979**, *12*, 1136.
- (13) Tékéli, P.; Lauprêtre, F.; Monnerie, L. *Macromolecules* **1983**, *16*, 415.
- (14) Connor, T. M. *Trans. Faraday Soc.* **1964**, *60*, 1574.
- (15) Valeur, B.; Jarry, J. P.; Geny, F.; Monnerie, L. *J. Polym. Sci., Polym. Phys. Ed.* **1975**, *13*, 667.
- (16) Jones, A. A.; Stockmayer, W. H. *J. Polym. Sci., Polym. Phys. Ed.* **1977**, *15*, 847.
- (17) Hall, C. K.; Helfand, E. *J. Chem. Phys.* **1982**, *77*, 3275.
- (18) Jones, A. A.; Robinson, G. L.; Gerr, F. E. *ACS Symp. Ser.* **1979**, *103*, 271.
- (19) Dejean de la Batie, R.; Lauprêtre, F.; Monnerie, L. *Macromolecules* **1988**, *21*, 2045.
- (20) Howarth, O. W. *J. Chem. Soc., Faraday Trans. 2* **1979**, *75*, 863.
- (21) Doddrell, D.; Glushko, V.; Allerhand, A. *J. Chem. Phys.* **1972**, *56*, 3683.
- (22) Heatley, F.; Cox, K. *Polymer* **1977**, *18*, 225.
- (23) Noggle, J. H.; Schirmer, R. E. *The Nuclear Overhauser Effect*; Academic Press: New York, 1971.
- (24) Scrivens, J. H.; Heatley, F. *J. Chem. Soc., Faraday Trans. 2* **1976**, *72*, 2164.
- (25) Heatley, F.; Wood, B. *Polymer* **1978**, *19*, 1405.
- (26) Ovenall, D. W. *Macromolecules* **1984**, *17*, 1458.
- (27) Bovey, F. A. *High Resolution NMR of Macromolecules*; Academic Press: New York, 1972; Chapter. 8.
- (28) Gronski, W. *Makromol. Chem.* **1976**, *178*, 3017 (1976).
- (29) Denault, J. Thèse de Ph.D. (Chimie), Université de Montréal, Montréal, Canada, 1986.
- (30) Gérard, A.; Lauprêtre, F.; Monnerie, L. *Polymer* **1994**, *35*, 3402.
- (31) Dejean de la Batie, R.; Lauprêtre, F.; Monnerie, L. *Macromolecules* **1988**, *21*, 2052; **1989**, *22*, 122; **1989**, *22*, 2617.
- (32) Helfand, E. *J. Chem. Phys.* **1971**, *54*, 4651.
- (33) Conway, B. E. *Ionic Hydration in Chemistry and Biophysics*; Elsevier: Amsterdam, 1981.
- (34) Bieze, T. W. N.; van der Maarel, J. R. C.; Eisenbach, C. D.; Leyte, J. C. *Macromolecules* **1994**, *27*, 1355.
- (35) Wolf, R. M.; Suter, U. W. *Macromolecules* **1984**, *17*, 669.

MA951502D